

High-Resolution Imaging of Ionic Domains and Crystal Morphology in Ionomers Using AFM Techniques

R. Scott McLean,* Marc Doyle, and Bryan B. Sauer

DuPont Central Research and Development, Experimental Station, Wilmington, Delaware 19880-0356

Received March 14, 2000; Revised Manuscript Received June 19, 2000

ABSTRACT: AFM methods were applied to resolve the surface and near-surface morphology of the ionic domains in Nafion membranes, Surllyn ionomers, and other ionomers. The ionic clusters were resolved by a new tapping AFM method where low oscillation amplitudes were used, and tip–ionic domain interactions were apparently able to dominate the signal allowing nanometer-level resolution of the domains. In other operating modes, the fluoropolymer crystal or aggregate domains were imaged using tapping AFM by the normal “stiffness” contrast. By sequential images taken under different AFM conditions, the “softer” fluorine-depleted regions were found to contain ionic domains in the same topographical areas, and the changes due to swelling by water were examined in one case. A third AFM operating mode was used to examine the composition in the outermost few angstroms of the surface. Data proving the existence of a very thin fluorine-rich “barrier” layer covering the entire surface of Nafion are obtained, and its relevance to vapor versus liquid water penetration is discussed.

Introduction

Continued interest in ionomers and ion-exchange membranes for applications such as the membrane chlor-alkali process, anhydrous HCl electrolysis, and proton-exchange membrane fuel cells has motivated the study of the details of their morphology and microstructure.^{1–3} The relationships between ionomer structure and performance characteristics such as ionic conductivity are the critical driving force for much of this research and provide the foundation for fundamental modeling work on these materials.^{4–11}

Synthetic work on novel ionomeric polymers has been motivated of late by the renewed interest in the commercialization of the proton-exchange membrane fuel cell (PEM-FC).³ The demands of this application are challenging as the ionomer membrane must exhibit high ionic conductivity in low-humidity environments, high thermal and oxidative stability, and low cost. While perfluorinated ionomer membranes have historically been the only polymers to meet these requirements, it is possible that the use of novel materials may come to pass. For example, ionomer membranes with better methanol impermeability are desired for direct methanol PEM-FCs.¹² To bring this about, a closer connection between ionomer structure and physical properties, in this case methanol diffusion and electroosmotic drag, is required.

The presence of ionic clustering in many of these materials including ethylene methacrylate ionomers, perfluorinated sulfonic acid,^{4–6} and carboxylic acid ionomers has been established.^{13,14} Detailed theoretical models for ionic clustering exist that describe small-angle X-ray and neutron scattering data, dynamic mechanical properties, and certain characteristics of ionic conductivity and electrochemical performance such as the hydroxyl ion exclusion properties of perfluorinated ionomer membranes used in the membrane chlor-alkali process.

Gierke et al.^{4,5,15} first proposed the cluster-network model for perfluorinated ionomers membranes which is still used to describe the fundamental relationship

between ionomer cluster structure and certain electrochemical characteristics of the ionomer.¹⁵ This model emphasizes the fact that the solvent swelling and ionic conductivity of these ionomers are dominated by the cluster network, while certain other characteristics such as anion exclusion and hydrodynamic permeability are dominated by intracluster transport processes. These latter processes are presumed to involve transport inside of “channels,” possibly cylindrical in nature, that connect adjacent clusters. This model continues to be the basis for fundamental modeling efforts¹⁶ ranging from macroscopic pore models⁷ to molecular dynamics studies.⁸

Further microstructural models of perfluorinated ionomer membranes have been based on a three-phase model.^{13,16,17} In this model, the ionomer consists of three regions: one being the hydrophobic fluorocarbon backbone region, the second being the hydrophilic ionic cluster region, and the third being an interfacial region with intermediate behavior. The hydrophobic fluorocarbon region is the location of any crystallinity that exists in the polymer while the hydrophilic region accommodates the majority of the absorbed solvent and hence is critical to ionic and solvent transport characteristics.

Studies of ionic cluster formation and its dependence on ionomer composition and environment have been based on scattering data where the presence and structure of clusters are inferred by fitting the scattering data to simple models.¹³ Direct experimental visualization of the clusters using, for example, dye-staining transmission electron spectroscopy (TEM) is challenged by the poor image contrast in perfluorinated ionomers and the need to create extremely thin membrane samples.¹⁸ In addition, the inherent flexibility of the polymer opens up the possibility of changes in polymer microstructure caused by the experimental methodology. Finally, the electron microscopy techniques cannot follow changes in the ionomer structure in-situ such as those caused by changes in environmental conditions.

Nonetheless, many TEM studies have been performed and have generally found evidence of small 3–10 nm

ionic clusters approximately spherical in shape.^{19–23} A recent dye-stained TEM study of a heavily sulfonated styrene-(ethylene-butylene)-styrene triblock polymer exhibited lamellar shaped ionic regions consistent with the phase-separated structure of the base polymer.²⁴

There exist a number of fascinating and important issues related to ionomer membrane surface structure. One pervasive and unexplained phenomenon is the difference in water uptake for perfluorinated ionomer membranes exposed to liquid water versus saturated water vapor under otherwise identical conditions. The presence of this difference has been referred to as Schroeder's paradox and continues to receive study due to the uncertainty in its resolution.^{25–27} Recent theories to explain this experimental finding postulate different regions in the membrane or different mechanisms for water uptake from the two environments. Another possible explanation that has support based on contact angle measurements involves changes in the surface morphology of the membrane exposed to the different environments.²⁸ The membrane interfacial region, especially the outermost few angstroms of the polymer surface, is also critical because it can present a substantial mass-transfer barrier, although the extent to which the interfaces dominate water transport in applications such as the PEM-FC is still controversial.

While much is known about ionomer structure and membrane transport properties from the above studies, there is still a pressing need for experimental techniques that can provide more detailed structural information at the nanometer level. If such information can be obtained in the presence of the solvent medium and under dynamic conditions, it should provide valuable information for future modeling work to further develop the connection between structure and transport properties.

Atomic force microscopy (AFM) can have the resolution required to elucidate polymer microstructural features at the nanometer scale. However, its application in the ionomer field to date has been relegated to examination of surface textural features rather than achieving the resolution and imaging techniques necessary to directly examine ionic clustering.^{29–31} The present study will demonstrate that it is possible to image ionic clusters in a number of different ionomer systems and also provide additional morphological information not available from any other real-space technique because of the ability of AFM to characterize the fluorine-rich crystal aggregates in addition to determining the relative morphological position of the ionic species and domains. The real space organization and network of ionic and nonpolar aggregates is relevant to transport and mechanical properties.^{4,15,16} Studies of nonionic polymers including the Nafion precursor polymer also serve as important controls in our efforts in assigning various phases.

Related and possibly better-characterized systems from the morphological standpoint are ionomers such as poly(ethylene-*co*-methacrylic acid) neutralized with Zn and other metal ions, which would be one example of the Surlyn family of copolymers. Morphologies in Surlyn and related materials have been studied by many techniques.^{32–36} Using scanning transmission electron microscopy (STEM),³⁶ recent studies have shown excellent resolution of the very small ionic domains. The diameters of the domains are approximately 2.5 nm for a Zn-neutralized Surlyn with slightly

higher acid content than that studied here and are characterized by a relatively low dispersity in domain sizes.³⁶ Although small-angle X-ray scattering (SAXS) provides some characterization of the organized fraction of ethylene lamellae, it is deficient in these complicated systems because of the low degree of perfection. The overall phase structure and organization including the polyethylene lamellae are not easily resolvable by electron microscopy because the ethylene crystals are imperfect. In addition to causing difficulties in resolving ethylene crystals by electron microscopy, the low degree of three-dimensional order contributes to a disparity in the total percent crystallinity derived from wide-angle X-ray diffraction which is lower than that derived from DSC in Surlyn type materials. On the basis of literature including recent AFM work on nonionic ethylene copolymers,³⁷ resolving and imaging these imperfect crystals should be possible with tapping AFM. Because the electron microscopy section thickness is not exactly controlled and is large relative to the ionic domain size, the position in space of ionic domains relative to the ethylene crystal aggregates (i.e., stacks of lamellae) is difficult to discern. Here we explore the application of AFM because to our knowledge no combination of imaging techniques applied to systems such as Surlyn and Nafion has demonstrated the characterization of the positions in space of the ionic domains relative to the crystal lamellae or lamellar stacks.

Experimental Details

Surlyn 1652 from DuPont is based on ethylene-*co*-methacrylic acid with 8.7 wt % acid and 18% of the acid groups neutralized with Zn. Nafion 117 membranes in sulfonyl fluoride precursor form had an equivalent weight¹⁵ of 1100 [i.e., $-(CF_2CF_2)_{6.5}-(CF_2CF(OCF_2CF(CF_3)OCF_2CF_2SO_2F))$]. They were hydrolyzed using 1.0 M KOH in a 2:1 mixture of deionized water:DMSO by heating at 60 °C for 2 h to give the ionic (K^+) neutralized sulfonic acid form. The membranes were rinsed extensively with deionized water and boiled in deionized water for 1 h and dried in a vacuum oven at 130 °C. Images were taken of both the sulfonyl fluoride precursor membrane and the K^+ -form ionomer under ambient humidity so the samples are certainly not free of water.

Samples of a sulfonated triblock polymer were received from the Dais Corporation (60% sulfonated Kraton G1650, PTFE reinforced films) sandwiched between cover sheets. The "G" series of Kraton polymers from Shell are triblock copolymers where the midblock (elastomeric) portion of the polymer is saturated. The G1650 base polymer is a triblock copolymer composed of styrene-(ethylene-butylene)-styrene. These films were used as-received for AFM imaging.

Smooth surfaces can improve resolution of nanocrystal structures in AFM studies. Obtaining smooth surfaces from the melt for polymers that crystallize can be difficult because crystallization in some polymers roughens the surface. Because of this we developed methods to fabricate very smooth surfaces for the ethylene-based ionomers. Thermal melt or "melt-pressed" surfaces were obtained by pressing a smooth silicon surface onto the Surlyn melt at 180–200 °C and cooling at 40 °C/min. Because of the low crystallinity of Surlyn, the AFM results on such surfaces were qualitatively consistent with samples prepared by cooling a free air melt surface. The Surlyn samples were not annealed at elevated temperatures after cooling.

Tapping mode AFM³⁸ was used to obtain height and phase imaging data simultaneously on a Nanoscope IIIa from Digital Instruments, Santa Barbara, CA. Microfabricated cantilevers or silicon probes (Nanoprobes, Digital Instruments) with 125 μ m long cantilevers were used at their fundamental resonance frequencies which typically varied from 270 to 350 kHz

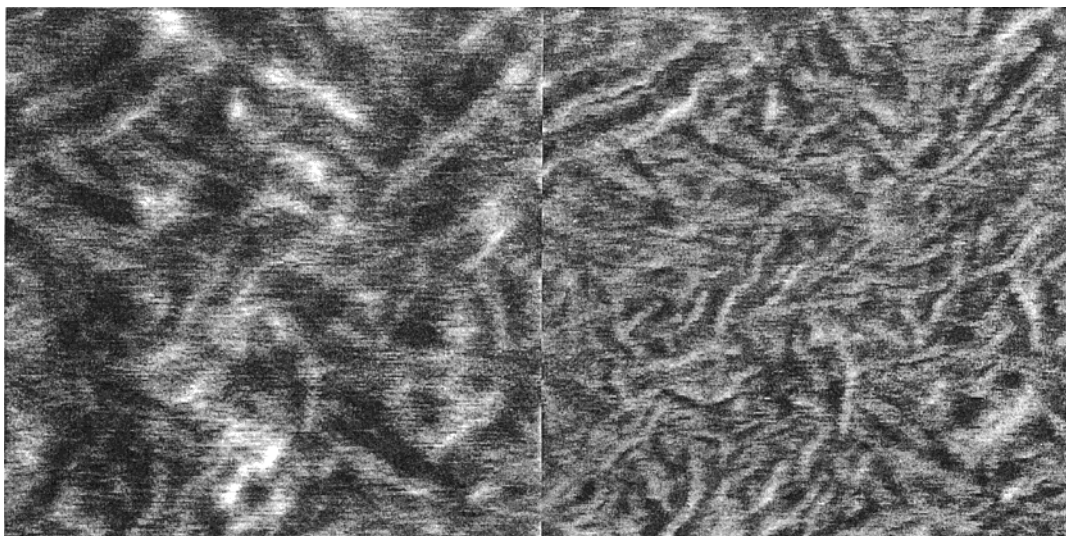


Figure 1. AFM “normal” tapping height (A) and “phase” (B) data for a Surlyn 1652 film surface. The height data on the left show short- and long-range roughness, and the phase data on the right give similar but better resolved details of lamellar morphology. The high spots are light and correspond to the hard regions in phase. Scan boxes are 250×250 nm for each plot, and the height and phase scales are 0–10 nm and 0–20°, respectively.

because of small variation from cantilever to cantilever. Very small tip radii (5–10 nm) are necessary for the ~ 1 nm lateral resolution needed for these studies. The AFM was operated in ambient with a double vibration isolation system. Extender electronics were used to obtain height and phase information simultaneously. The lateral scan frequency was about 1.5 Hz. The images presented here are not filtered.

In tapping mode where the tip makes intermittent contact with the surface, the level and method of applying the force to the surface can dramatically change the data in the regime where no surface damage is occurring, especially the phase data. Tapping AFM dramatically reduces lateral drag forces^{38,39} which can become high with these very sharp tips in standard contact AFM. These tapping forces are roughly adjusted by the “amplitude ratio” ($R = A_{\text{eng}}/A_{\text{free}}$) of the engaged (A_{eng}) or set point amplitude to the free air amplitude (A_{free}), keeping the frequency relative to the resonance peak controlled on the low-frequency side,^{40,41} to avoid artifacts. This is typically not well controlled in the literature. This ratio of amplitudes which are used in feedback control was adjusted to $R = 40$ –70% of the free air amplitude ($A_{\text{free}} \sim 50 \pm 10$ nm) for “moderate force” imaging.^{38–40} Under these “normal” tapping conditions, phase lag data are sensitive to local stiffness differences of species or domains in the top several nanometers from the outermost surface,^{39,40} and from knowledge of polyurethane composition we can indirectly estimate that normal tapping can detect domains down to about 10 nm below the surface.³⁹ Harder domains have a larger phase lag and will be plotted as the light regions.^{39,40}

New imaging conditions reported here were designed to resolve the ionic domain morphology in both Surlyn and Nafion ionomers. We found that, by operating at lower amplitudes of oscillation of about 8 ± 3 nm, phase lag data that are insensitive to stiffness can be obtained with appropriate experimental control. This lower energy applied to the cantilever allows one to directly image the ionic clusters at or near the surface. Our interpretation is that lowering the oscillation amplitude of the cantilever allows attractive tip interactions with the polar ionic domains to dominate the AFM phase signal, giving rise to relatively high contrast in the absolute magnitude of the phase shift. As discussed below, the nonionic sulfonyl fluoride Nafion precursor and many other controls were used to prove that polar domains cannot be detected unless they contain ionic species in Nafion and related materials in this low oscillation amplitude mode. The ratios of tip oscillation amplitudes (R) for low oscillation amplitude imaging conditions were adjusted to the same ratios as for our normal tapping conditions. If ionic regions have the same

“stiffness” as amorphous polyethylene, then we should not expect any contrast with AFM in normal “phase” imaging as is verified later.

Finally, a very light tapping force method demonstrated recently in our laboratory⁴² was used to look for polar domains or contrast based on hydrophobicity differences at the outer few angstroms of the surface, i.e., a closer to true surface-specific imaging technique. This mode is implemented by keeping the oscillation amplitude the same as in normal tapping (i.e., 50 nm) but increasing R substantially to about 0.9 ± 0.05 , which reduces the tip to surface interaction forces substantially.^{38,41,42} Ionic species are not required for contrast in this mode and actually generally do not even contribute because the technique is so surface specific and the ionic domains are usually buried to a certain degree. Only hydrophobicity differences are needed, and these can come from a variety of sources. This technique was applied recently to nanoresolution of hydrocarbon–fluorocarbon mixed surfaces and other related model systems.⁴²

A brief summary of the AFM phase imaging methods and their approximate probe depths normal to the plane of the surface is as follows:

1. Normal tapping under moderate forces uses stiffness contrast to resolve domains from the top surface down to about 5–10 nm into the bulk.
2. Low oscillation amplitude tapping resolves ionic domains down to ~ 0 –5 nm below the surface. This method is a new method and is reported here for the first time. We have verified it with Nafion, Surlyn, and a number of control samples. Ionic species are necessary for contrast in this method of imaging.
3. Very-light tapping⁴² is sensitive to hydrophobicity differences in the outer 0.2–1.0 nm of the surface, and stiffness contrast contributions are negligible. Ionic species are *not* necessary for contrast and in fact have not been detected in this mode under ambient conditions because they are probably buried approximately 1 nm below the surface due to their high surface energies. Certain rough surfaces cannot be studied in this mode because the forces are so low that engagement with the surface can be lost as the tip scans over rough edges.⁴² Roughness was not a problem with Nafion membranes or with most Surlyn samples.

Results

Surlyn Ionomer Films. Simultaneously obtained AFM height and phase data for Surlyn 1652 were obtained under normal tapping conditions (Figure 1).

The total scan boxes shown in the figure are 250×250 nm. Discussions of how the phase data are sensitive to regions of different local stiffness were given earlier,^{38,39} in all plots white is high in topography and high in phase, and high phase indicates high stiffness regions in normal tapping. The ionic domains are not sensed or imaged in these data obtained under normal tapping conditions, although one would expect that they reside outside of the hard crystal "lamellae" in certain softer (darker) amorphous phase regions. The ethylene lamellae are relatively distinct as the higher regions in height (Figure 1A) and phase (Figure 1B) and some organization into parallel orientations are seen. As with most polymers of this type,³⁹ the outermost layer of the surface is covered with about 1 nm of amorphous material. For Surlyn, mostly amorphous polyethylene segments are the low-energy component and probably dominate the outermost surface. We must image through this layer, and one must consider that this may lower the contrast and sharpness of boundaries of the lamellae below the surface, as will their orientation relative to the plane of the surface.

For the most part we have determined crystal dimensions from the phase data and have found lamellae thicknesses approximately 6 ± 1 nm for the majority of the lamellae (Figure 1A), consistent with small-angle X-ray data.³³ The lengths are typically between 50 and 100 nm, and this quantity is not available from SAXS. The amorphous interlayer thickness between parallel lamellae is about 5 nm, and broader noncrystalline gaps in regions that have less ordered lamellae are typically much larger in dimension than 5 nm (Figure 1). As will be shown next, these "gaps" of softer material are also rich in ionic species and domains. This latter information is somewhat unique to real-space characterization techniques.

If ionic regions have the same "stiffness" as amorphous polyethylene, then we should not expect any contrast from ionic domains with AFM in normal "phase" imaging. This is the case in Figure 1B. Figure 2 shows phase images sequentially taken under normal (A) followed by low oscillation amplitude (B) conditions. The same 250×250 nm spot was studied in this comparison, and no height data are given. Normal tapping is sensitive to stiffness differences, showing mainly the lamellar organization in Figure 2A. In Figure 2B the contrast is derived from ionic concentration differences near the surface. To help guide the eye, we have provided arrows that show the soft regions where lamellae are absent (A), compared to the identical points in (B) that correspond to bright regions rich in ionic domains. The position of the arrows is performed on the instrument computer where exact corresponding locations can be determined, and other controls were performed to ensure that thermal drift did not contribute. Most ionic domains are clustered into these white regions and cannot be individually resolved in (B) because they are overlapped with each other. Many separate ones are resolvable as small white dots in Figure 2B (several are in the box near the bottom) and have diameters on the order of ~ 2 nm, consistent with recent SAXS data and analysis which extract a diameter of 1.7 nm for a slightly different Surlyn material and with high-resolution scanning TEM where diameters of about 2 nm are found. The contribution of interphase species and possibly reduced resolution due to the depth of the ionic domains beneath the hydrocarbon layer

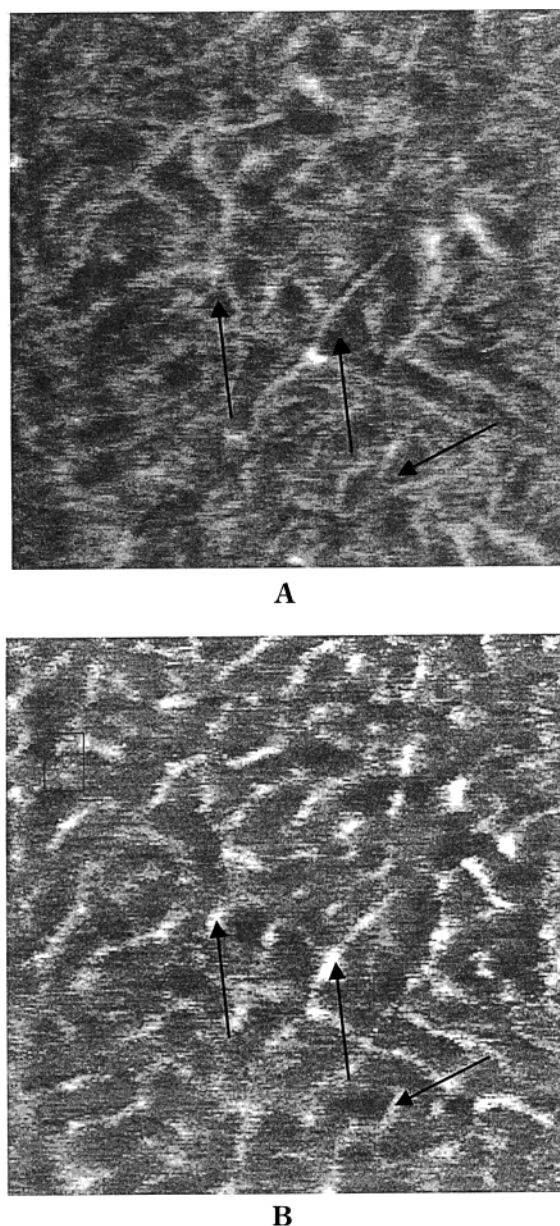


Figure 2. Phase images of a Surlyn 1652 surface in AFM normal (A) and low-energy (B) tapping. No height data are shown. Normal tapping is sensitive to stiffness contrast, and low-energy tapping derives its contrast from ionic-rich regions just below the surface (see text). Sequential images were taken on identical spots using the two conditions. Arrows indicate representative soft (dark) regions in the phase data (A), and the exact corresponding spots showing high populations of ionic species (light) in low-energy tapping (B). Part B shows one boxed region where several individual ionic domains are barely resolved with diameters on the order of 2–3 nm. Scan boxes are 250×250 nm with scales of $0-15^\circ$ and $0-80^\circ$ for (A) and (B), respectively.

make the AFM data qualitative. Higher magnification scans do not improve the resolution of single ionic domains significantly possibly because of larger degrees of sample deformation because of the higher residence time of the tip on the surface.

Nafion Perfluorinated Ionomer Membranes. In ethylene copolymers such as Surlyn, the metal neutralized form exhibits nanophase separation into small ionic domains as seen in Figure 2B, while the acid (H^+) form without metal neutralization does not exhibit distinct polar domain phase separation.³³ Because sulfonic acid

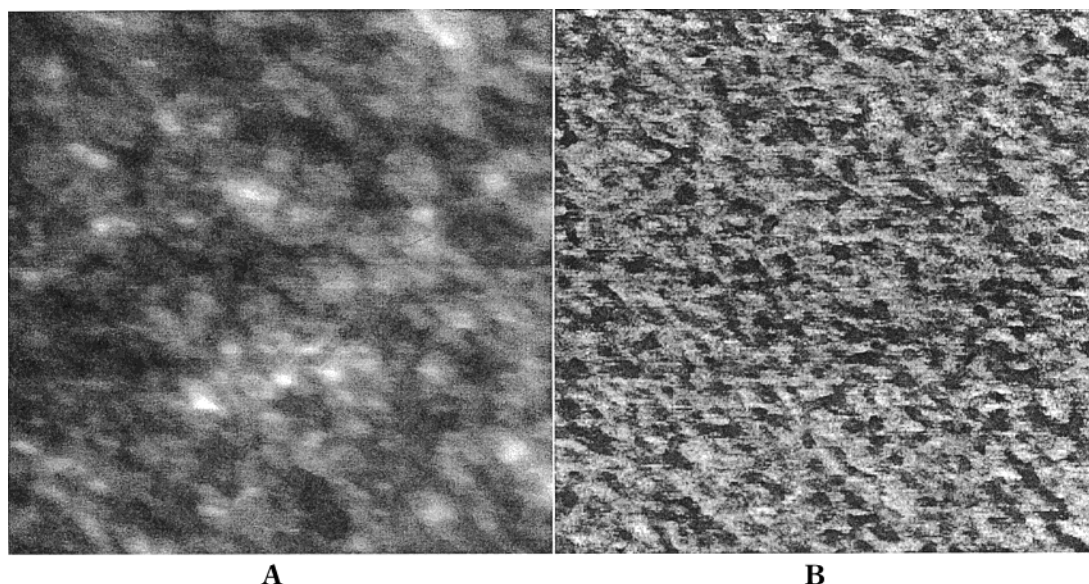


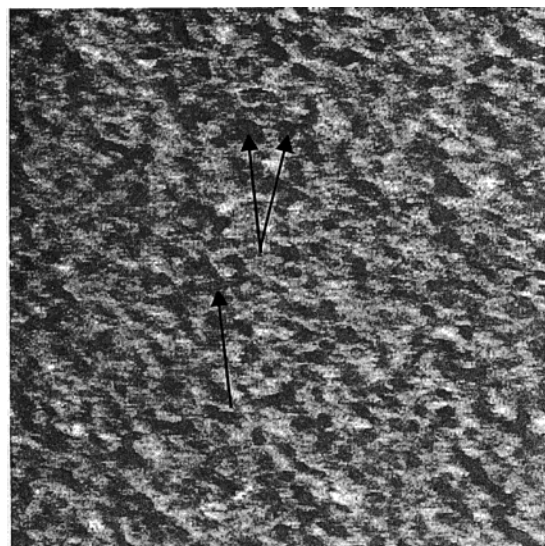
Figure 3. AFM normal tapping force height (A) and "phase" (B) data for a Nafion 117 (K^+) ionomer membrane surface. Scan boxes are 300×300 nm for each plot, and the height and phase scales are 0–10 nm and 0–20°, respectively.

is a much stronger acid than carboxylic acid, both acid (H^+) and metal neutralized acid forms of Nafion membranes exhibit strong nanophase separation into ionic domains. AFM data (total scan boxes shown are 300×300 nm) show high local regions in Figure 3A for Nafion 117 (K^+), which correspond to the stiff (light) regions in the phase data (B) taken simultaneously, both using normal tapping conditions. These stiff regions are the fluorocarbon crystalline domains. The phase data taken under normal tapping conditions sense stiff domains from the outermost surface down to about 5–10 nm below the surface,³⁹ so the light gray regions are the stiffer crystalline regions detected within this distance of the surface.

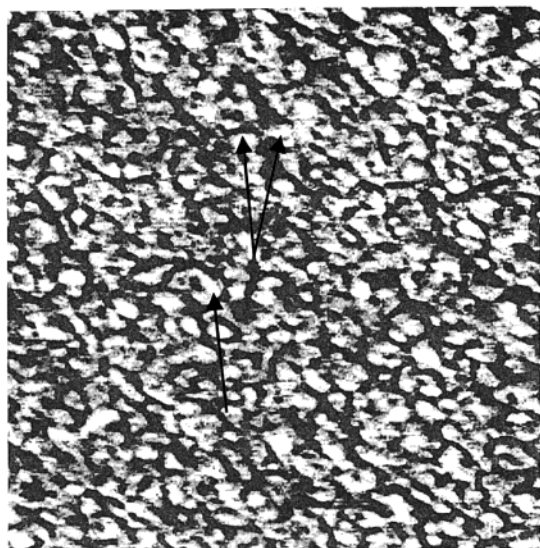
Similar to Figure 3B, high magnification normal tapping phase data (total scan boxes shown are 300×300 nm) for Nafion 117 (K^+) ionomer exhibit light gray regions which are the stiffer fluorocarbon crystalline regions closest to the surface (Figure 4A). No height data are shown in Figure 4. The approximate surface area coverage of light (stiff) regions in these normal tapping phase data is about 60% (Figure 4A), a value somewhat larger than the nominal crystal volume fraction in this material of about 30%. This higher apparent surface fraction is simply due to the finite probe depth of AFM where domains are detected down to about 5–10 nm below the surface³⁹ and naturally give apparent area fractions greater than the bulk. From our understanding of surface energies and contact angle data discussed later, a fluorocarbon layer probably dominates the entire outermost several tenths of a nanometer of the surface.²⁸ The approximate diameters of the crystalline domains vary, but for the better resolved domains in Figure 4A dimensions are on the order of 10 nm (100 Å) consistent with previous TEM^{21,23} and AFM^{29,30} results. The domains are less distinct and have lower anisotropy than the polyethylene-like lamellae in Surllyn perhaps because of a higher volume fraction of noncrystallizable species, shorter available TFE block lengths in Nafion, or a higher degree of undercooling during crystal formation.³⁵ Higher temperature annealed samples have not yet been studied.

In normal tapping, hard domains detected further below the surface will have lower contrast, so it is possible that some of the "crystals" are covered by several angstroms of amorphous and even partially ionic species. The darkest (black) regions are the softest regions (Figure 4A) and presumably contain the amorphous fluorocarbon and ionic-rich regions. Also, very-light tapping data obtained using the technique described previously⁴² show no contrast indicating that the outer few angstroms of the surface are relatively uniform in lateral composition, i.e., a thin surface excess layer of fluorocarbon exists. These very-light tapping data are featureless and are not shown here but are described under method 3 in the AFM technique summary in the Experimental Section.

Figure 4B shows a phase image taken using the low oscillation amplitude method 2 (see Experimental Section) on the same spot immediately after the data in Figure 4A were acquired. The white areas are the regions rich in ionic domains, and the dark areas are the regions where the ionic groups are absent or depleted. Such contrast in this low oscillation amplitude AFM mode is absent in the film of the sulfonyl fluoride Nafion precursor (Figure 5B), confirming that ionic domains are necessary for contrast. The sulfonyl fluoride Nafion also has no SAXS peak because polar group phase separation into distinct domains does not occur. Many controls were performed on various nonionic polymers exhibiting nanophase-separated domains, showing no such contrast in low oscillation amplitude tapping. The white regions in Figure 4B correlate with the dark regions in Figure 4A (corresponding spots are indicated by the arrows), showing that much of the softer matrix in Figure 4A is rich in ionic species. Normal tapping phase data in Figure 5A show that there is some contrast due to stiff lamellae in the nonionic sulfonyl fluoride Nafion polymer as expected since it is characterized by a finite level of crystallinity, and this stiffness contrast is similar in Figure 5B. A similar picture in Surllyn is found except the crystalline morphology has a higher degree of organization, and the ionic domains are sometimes excluded from the small stacks of ethylene lamellae. Stacks are defined



A

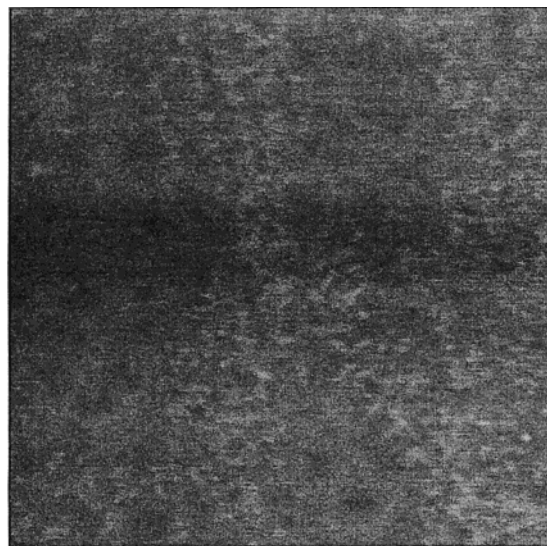


B

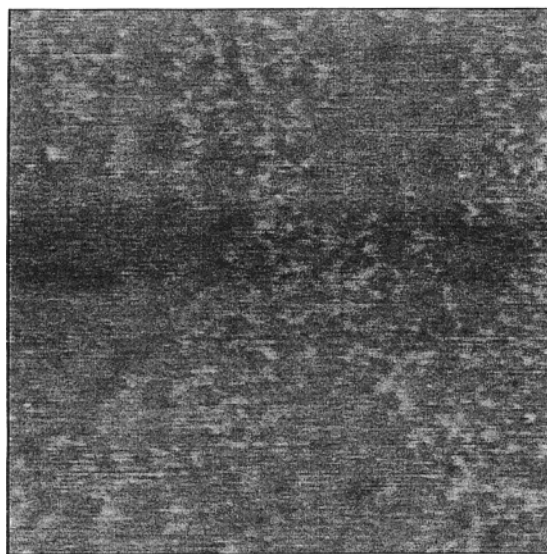
Figure 4. Images of Nafion 117 (K^+) ionomer membrane surface in AFM normal (A) and low oscillation amplitude (B) tapping. No height data are shown. Normal tapping is sensitive to stiffness contrast, and low-energy tapping has contrast from ionic-rich regions. Only phase data are shown for the two identical imaged regions. Arrows indicate representative soft (dark) regions in the phase data (A) and the exact corresponding spots showing high populations of ionic species (light) in low-energy tapping (B). Scan boxes are 300×300 nm with a phase range in (A) of $0-10^\circ$ and (B) of $0-40^\circ$.

as arrays of approximately parallel oriented lamellae, and some of these features are schematically illustrated in Figure 6 for Surlyn. "Stacks" are not present in our images of the 1100 equivalent weight Nafion membrane samples.

The size of the few smaller discrete white dots is 4–5 nm in Figure 4B, consistent with morphological characterization of ionic domain size by TEM,^{21,23} and the larger white regions are presumably clumps of overlapped ionic domains which cannot be individually resolved by AFM. SAXS has good contrast for ionic domains,^{15,20,21,33} giving diameters on the order of 3 nm for "dry" samples, so the lack of distinct boundaries in AFM is either due to overlap of domain boundaries beneath the surface contributing to a lack of AFM



A



B

Figure 5. Phase images of a Nafion sulfonyl fluoride (nonionic form) membrane surface in AFM normal (A) and low oscillation amplitude (B) tapping. No height data are shown. This nonionic material is used as a "control". Scan boxes are 1000×1000 nm for each plot, and phase range $0-30^\circ$.

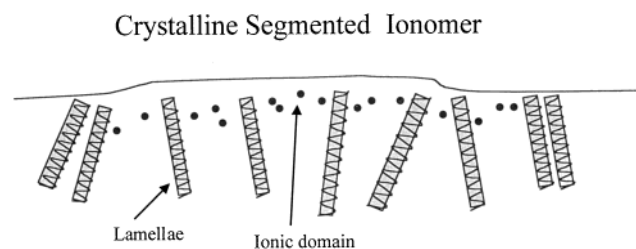


Figure 6. Schematic of Surlyn surface morphology.

contrast or because ionic species may be contained in the interphase regions between ionic domains, and AFM may not have sufficient contrast in such a situation. The spatial resolution of AFM is high enough, but due to the complicated mechanisms of imaging of domains just below the surface, we cannot quantify these contributions. The data also confirm that there is no observable stiffness contrast between ionic domains and the other amorphous phases in normal tapping; thus, there is

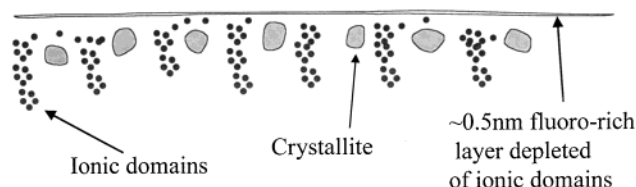


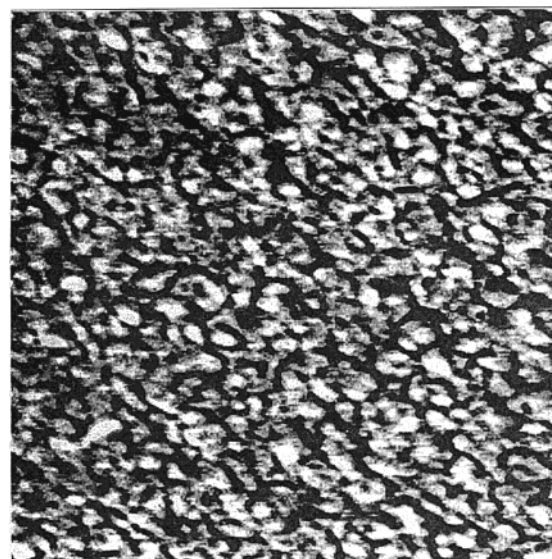
Figure 7. Schematic cartoon of Nafion surface morphology based on AFM studies.

no resolution of ionic domains in the normal tapping phase data in Figure 4A. Also, the data in Figure 4B show that the contrast of hard fluorocarbon domains in the low oscillation amplitude tapping mode is negligible compared to the ionic domain contrast, and this is consistent with the Surlyn results (Figure 2).

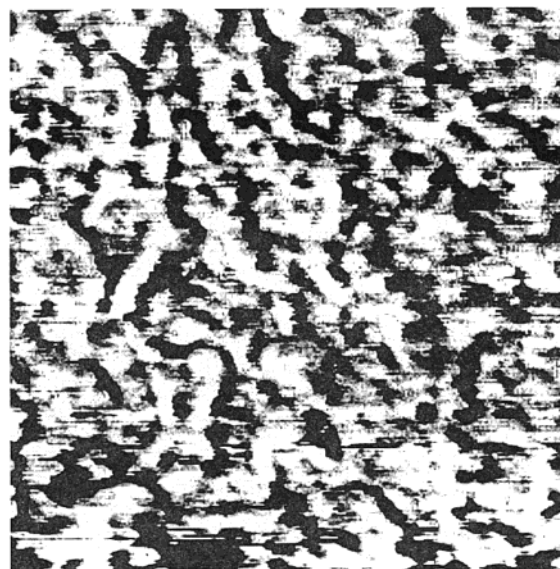
On the basis of the very-light tapping data discussed above and contact angle data discussed later, the AFM technique used to obtain the data in Figure 4B images through a thin fluorocarbon-rich layer in order to detect the ionic domains when the membrane is imaged under ambient (air) conditions as in this work. The maximum probe depth for ionic species with this low oscillation amplitude method is probably about 5 nm. Thus, in the black regions the fluorocarbon crystals extend at least a few nanometers beneath the surface, which is not surprising since the crystals are quite large (~ 10 nm in dimension in Figure 3B and ref 15). Figure 7 is a schematic illustration of the surface morphology in Nafion with domain sizes approximately to scale. The three different modes of AFM phase imaging used here were used to characterize or estimate all these features consisting of stiff fluorocarbon domains, clumps of ionic domains, and a thin surface excess layer containing mostly fluorocarbon with minimal ionic species.

Because the membranes are utilized for electrochemical applications in the presence of electrolyte solutions or solvents, the morphological responses to solvent swelling have been extensively examined by SAXS.^{5,15,20,21} Using low oscillation energy AFM to resolve ionic domains, Figure 8A shows phase data only for typical ambient humidity conditioned Nafion 117 (K^+) exhibiting a high level of uniformly spaced ionic domains or clumps of multiple (unresolvable) ionic domains with a clump size of about 4–10 nm in diameter. Because of the contrast in this AFM mode, the ionic species are contained in the light regions. Figure 8B shows phase data for a representative surface region on the same system after soaking in liquid deionized water. The contrast is high between fluorocarbon and ionic-rich regions; the clumps of ionic domains have approximately doubled in size to 7–15 nm in the narrow dimension, and most of the clumps of domains appear more like large channels making up the ionic cluster rich phase. The change in dimensions seen by AFM are roughly consistent with a bulk swelling of 50 vol %.¹⁵ Gierke et al.¹⁵ have estimated that each ionic domain swollen to about 5 nm diameter contains about 1000 water molecules, corresponding to about 20 water molecules per ionic group in water saturated 1100 equivalent weight Nafion membranes. The height data, which are not presented here, show about a 2 times higher roughness, and the ionic-rich clumps consistently have a height of about 1 nm after swelling.

Dais Sulfonated Triblock Ionomer. The final system studied is substantially different in composition. A sulfonated triblock copolymer composed of a styrene–(ethylene–butylene)–styrene base polymer was ob-



A

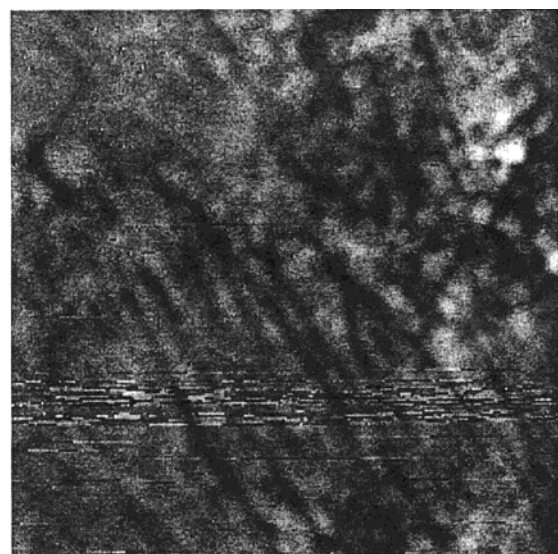


B

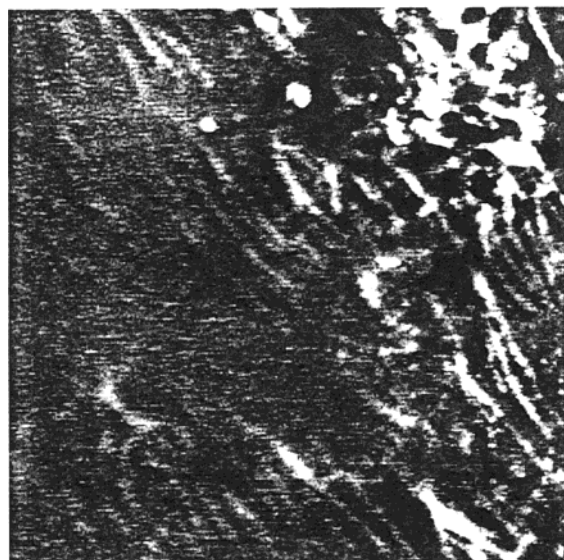
Figure 8. Low-energy phase images of Nafion 117 (K^+) ionomer membrane after exposure to room temperature humidity (A) versus deionized water exposure (B). Only phase data are shown, and scan boxes are 300×300 nm with a scale of $0-80^\circ$.

tained in acid form and used as received. The triblock copolymer is well-known to form a cylindrical or lamellar structure. Dye-stained TEM images confirm that the sulfonated ionomer also forms a lamellar structure with a spacing of approximately 25–30 nm.²⁴

AFM images shown in Figure 9A also confirm the lamellar structure of the sulfonated triblock copolymer. The scan boxes shown in Figure 9 are 1000×1000 nm. The domain spacing illustrated in this figure is similar to that found from the TEM images, being approximately 20–30 nm. Figure 9A suggests that alternating hard and soft regions exist in the sulfonated ionomer, although we cannot say conclusively that the sulfonated styrene segments remain the hard segment. Comparison with the low oscillation amplitude tapping data in Figure 9B suggests that the ionic regions may originate from the “soft” regions in Figure 9A. However, there is some uncertainty in this conclusion as not all features



A



B

Figure 9. AFM phase images of a triblock sulfonated polystyrene copolymeric ionomer from Dais Corporation in AFM normal (A) and low-energy (B) tapping. No height data are shown. Identical areas were imaged using the two conditions. Scan boxes are 1000×1000 nm with phase ranges of $0-20^\circ$.

line up well in the computer analysis comparing specific areas. Future work is needed to fully understand this material.

Discussion

Small-angle X-ray scattering is the technique most commonly used to characterize both the ionic clusters and the lamellar crystals of the hydrocarbon segments in metal neutralized Surlyn polymer samples.³²⁻³⁵ AFM images in Figure 2 and the resulting schematic in Figure 6 suggest that there is some level of exclusion of ionic domains from crystal lamellae as is expected because the crystals could not exist if they contained ionic domains. These data also suggest that ionic domains are at least partially excluded from the thin amorphous layers between stacked lamellae, even though the lamellar stacks are admittedly imperfect in the Surlyn studied here. Register and Cooper³³ have proved

by SAXS, where electron densities of the various phases were estimated, that there are some ionic species between stacked lamellae, but maybe the mobility is restricted enough that full ionic domains cannot form in these regions. More work on these systems with different thermal histories is required to fully understand this level of detail. Because of exclusion from crystal phases and/or exclusion from entire stacks of oriented lamellae, the ionic domains are clustered together (Figure 6). SAXS gives 1.7 nm diameter domains and a long period (average spacing from center to center) equal to 2.8 nm.³⁴ STEM gives diameters of 2.5 nm with a somewhat larger spacing between domains, and these values are less subject to problems with interpretation.³⁶ Part of the cause of the close to space-filling nature of the ionic domains is the exclusion from the crystalline domains, causing a concentration of ionic domains outside of the lamellar regions as confirmed by AFM. Gierke et al.¹⁵ have also characterized the close to space-filling nature of ionic domains in the ionic-rich regions in many Nafion membrane systems.

The approximate homogeneous dispersion in space shown by STEM techniques applied to Surlyn³⁶ can actually be contrasted with AFM, which shows that the ionic domains may be excluded into the broader amorphous regions between stacks. Recent models assumed that the ionic domains are in an amorphous phase well dispersed between lamellae,³³ and future AFM work will address the morphology in Surlyn ionomer resins exhibiting higher degrees of crystalline organization since our Surlyn in Figure 2 does not really exhibit well-defined multiple stacking of lamellae in parallel orientations.

In Nafion membranes, the crystal organization is such that individual lamellae are imperfect²³ and are not organized into stacks (Figure 7) at least for the sample preparation used here. As with Surlyn, ionic species are excluded from the crystalline domains, causing a concentration of ionic domains in a continuous noncrystalline phase characterized in some detail by AFM (Figure 4B). Because the ionic domains are concentrated outside of the lamellae, this also naturally explains some of the confusion in the literature regarding the higher apparent rate of swelling of the domains which contribute to the SAXS signal relative to the rate of volume change of the bulk polymer during solvent swelling.^{20,21} The likely change in the number of domains during swelling by solvents would also resolve some of the controversy.

For the purpose of discussion, we refer to the model of Gierke et al.^{5,15} where an inverted micelle type of structure approximately describes the spherical domains of ionic species. Because of the copolymer structure of Nafion, crystallization is frustrated, leading to relatively low crystallinity for the 1100 equivalent weight membrane. The fluorine-rich species that cannot be accommodated in crystals are partially interphase species at the surfaces of ionic domains. There is some mobility so these can rearrange and respond to external forces from permeants. Figure 8B showed the swelling of the clumps of ionic domains in broad and somewhat continuous channels between fluorocarbon lamellae, and SAXS shows the dimensional changes of the ionic domain spacings with swelling.¹⁵ The SAXS contrast between domains usually remains good under these conditions, and this is an advantage over AFM even

though there is much controversy concerning whether the SAXS signal is related to the interdomain spacing or the intraparticle dimension.^{15,20,21,33} The former is more likely for a variety of reasons.

Finally, the schematic in Figure 7 does not address the mechanism of bulk transport of permeants or ions in Nafion polymers.^{15,16} We presume that interfacial tension will drive the ionic domains toward a spherical shape; concentration fluctuations may be related to temporary formation of narrow channels connecting domains,^{5,15} or rearrangement of interfacial species could provide a continuous pathway. Interfacial tension would tend to restrict the formation of high surface area narrow channels and also tend to drive the system to larger ionic domain dimensions with the ultimate dimension limited mainly by steric chain factors. Polar interfacial species have also been considered in the modeling of transport¹⁶ in an extension of the model of Gierke et al. Figure 8B suggests that large clumps of ionic domains accumulate between lamellae in a continuous network leading to a pathway for polar penetrants. After these domains have been swollen, it is likely that polar permeants such as ions and polar solvent molecules would only have to diffuse across the thin amorphous or interfacial regions between swollen polar domains to proceed along these pathways. This is consistent with the low ionic and diffusional resistance of these ionomers in their swollen state.

Surface Morphology and Relevance to Contact Angles and Transport. First consider the Nafion membrane surface morphology consisting of ~10 nm diameter partially crystalline fluorine-rich domains which are complete barriers to water under all environments, combined with some coverage (~50%) of ionic-rich domains near the surface (Figure 7). AFM evidence presented above suggests that these ionic-rich domains are covered by a thin fluorine-rich "membrane";²⁸ typically these excess membrane layers of low surface energy species are formed because of surface tension driving forces and are on the order of 1 nm thick (Figure 7). The fluorine-rich layer is of unknown composition, but from advancing contact angles could be almost pure fluorocarbon, but this is not conclusive.²⁸ AFM results obtained with very-light tapping and described above verify that there are essentially no ionic species at the outermost few angstroms of the surface and, combined with the low oscillation amplitude AFM data (Figure 4B), prove that the concentration of ionic species is substantially greater just under the surface.

If we consider the response of Nafion membranes to liquid water exposure, the fluorocarbon groups are repulsed from the polar environment, and the ionic species are immediately attracted and "diffuse" to the outermost few angstroms of the surface. They can then facilitate rapid diffusion of water into the bulk of the Nafion film. The rearrangement time is quite fast (see discussion of Surlyn below) and probably occurs in less than a second²⁸ due to the high concentration of ionic species and high mobility of both ionic species and fluorocarbon species in the thin fluorocarbon excess layer.

The paper by Zawodzinski et al.²⁸ concludes from contact angle and liquid water and other water vapor aging studies that a thin fluorine-rich "membrane" layer acts as a barrier to water during vapor state exposure to the Nafion surface. This model seems correct, and the barrier to water vapor is likely the approximately

0.2–1.0 nm surface excess layer of fluorocarbon discussed above. Contrary to the case of liquid water or other polar liquid exposure, vapor exposure cannot cause a depletion of the fluorocarbon excess layer because the attractive force for driving ionic species migration to the surface is low because of the relatively low water mole fraction in the vapor phase. Thus, water vapor molecules from the outside are repulsed by the hydrophobic surface and cannot entirely diffuse into the bulk.

In Surlyn the ionic species take substantially longer to migrate the nanometer to the surface because they are at a lower volume fraction, and they consist of more discrete domains covered by a complete layer of hydrocarbon in the typical Surlyn film. There may also be a lower driving force relative to motion of ionic domains in Nafion due to the higher enthalpy of interaction of sulfonic acid groups with water. Contact angles on fresh Surlyn surfaces show essentially identical results to polyethylene because of the slow rearrangement time of the surface species. Upon exposure to polar liquids, mainly buffered salt solutions, ionic species slowly migrate to the interface, and the results on Surlyn show continuous increases in surface concentration of ionic species at the surface over a period of 24 h, with the majority of the increase occurring within the first hour. This is contrasted with the very rapid response of Nafion to liquid water, on the order of seconds or less.²⁸

Conclusions

AFM methods were applied to resolve the surface and near-surface morphology of the ionic domains in Nafion membranes, Surlyn ionomer resin, and other ionomers. A new AFM method was developed and applied here to detect the ionic domains near the surface. This was implemented by using low oscillation amplitudes where tip–ionic cluster attractive interactions were found to dominate the signal, facilitating nanometer-level resolution of the ionic domains. In other "standard" operating modes, the fluoropolymer aggregate (crystallites) domains could be imaged by tapping AFM using normal "stiffness" contrast. By sequential images taken under different AFM conditions, the "softer" fluorocarbon depleted regions were found to contain ionic domains in the same topographical areas. AFM has the advantage that the dimensions and anisotropy of the lamellae or crystallites are determined in real space in addition to the dispersity in sizes and the relative positions and orientations in space.

The morphology of Surlyn consists of some parallel organization of ethylene lamellae into imperfect stacks with ionic domains partially segregated into regions outside of the lamellar stacks in these low crystallinity systems containing imperfect crystal organization. Stacks (or fibrils) are defined as small regions of approximately parallel lamellae. The morphology of Nafion consists of nonstacked individual fluorocarbon crystallites separated by a matrix containing the ionic domains that are in the form of clumps of many possibly individual domains not easily resolved by AFM. This is contrasted with SAXS techniques where individual ionic clusters are relatively well resolved.

In both Nafion and Surlyn the data support the model of Gierke et al.^{5,15} where an inverted micelle type of structure approximately describes the spherical aggregates or domains of ionic species. Other models

cannot be ruled out, but there is no evidence for domain shapes other than approximately spherical in these ionomers. One Nafion membrane sample was swollen with water and AFM used to evaluate the expansion of the ionic-rich regions. Clear signs of expansion of the individual clusters as well as the clumps of clusters were seen. Clumps of clusters appear to converge in the AFM images into longer structures that may improve connectivity and provide better pathways for protons and water through the swollen ionomer. The formation of the clumps were controlled by the neighboring fluoro-carbon crystallites.

Sulfonated triblock copolymer images showed a lamellar structure with a periodic repeat distance of 20–30 nm, consistent with TEM images from the literature on this polymer. Ionic domains with similar lamellar structure and dimension were found in the low oscillation amplitude tapping AFM mode. The ionic regions may exist in the soft regions of this copolymer, but the results are not conclusive.

Acknowledgment. We thank Drs. D. Londono, S. Mazur, and K. Stika for their important contributions.

References and Notes

- (1) Pourcelly, G.; Gavach, C. In *Proton Conductors, Solids, Membranes, and Gels-Materials and Devices*; Colomban, P., Ed.; Cambridge University Press: Cambridge, 1992.
- (2) Heitner-Wirguin, C. *J. Membr. Sci.* **1996**, *120*, 1.
- (3) Savadogo, O. *J. New Mater. Electrochem. Syst.* **1998**, *1*, 47.
- (4) Gierke, T. D.; Hsu, W. Y. In *Perfluorinated Ionomer Membranes*; Eisenberg, A., Yeager, H. L., Eds.; ACS Symposium Series No. 180; American Chemical Society: Washington, DC, 1982; Chapter 13, p 283.
- (5) Hsu, W. Y.; Gierke, T. D. *J. Membr. Sci.* **1983**, *13*, 307.
- (6) Wodzki, R.; Narebska, A.; Nioch, W. K. *J. Appl. Polym. Sci.* **1985**, *30*, 769.
- (7) Verbrugge, M. W.; Pintauro, P. N. In *Modern Aspects of Electrochemistry*; Conway, B. E., Bockris, J. O'M., White, R. E., Eds.; Plenum Press: New York, 1989; Vol. 19.
- (8) Din, X.-D.; Michaelides, E. E. *AIChE J.* **1998**, *44*, 35.
- (9) Paddison, S. J.; Reagor, D. W.; Zawodzinski, Jr., T. A. *J. Electroanal. Chem.* **1998**, *459*, 91.
- (10) Paddison, S. J.; Zawodzinski, Jr., T. A. *Solid State Ionics* **1998**, *113–115*, 333.
- (11) Paddison, S. J.; Pratt, L. R.; Zawodzinski, Jr., T. A. *J. New Mater. Electrochem. Syst.* **1999**, *2*, 183.
- (12) Ravikumar, M. K.; Shukla, A. K. *J. Electrochem. Soc.* **1996**, *143*, 2601.
- (13) Eisenberg, A.; Kim, J.-S. *Introduction to Ionomers*; John Wiley & Sons: New York, 1998.
- (14) Mauritz, K. A. *J. Macromol. Sci., Rev. Macromol. Chem. Phys.* **1988**, *C28* (1), 65.
- (15) Gierke, T. D.; Munn, G. E.; Wilson, F. C. *J. Polym. Sci., Polym. Phys.* **1981**, *19*, 1687.
- (16) Yeager, H. L.; Steck, A. *J. Electrochem. Soc.* **1981**, *128*, 1880.
- (17) Eisenberg, A.; Hird, B.; Moore, R. B. *Macromolecules* **1990**, *23*, 4098.
- (18) Handlin, D. L.; MacKnight, W. J.; Thomas, E. L. *Macromolecules* **1981**, *14*, 795.
- (19) Ceynowa, J. *Polymer* **1978**, *19*, 70.
- (20) Fujimura, M.; Hashimoto, T.; Kawai, H. *Macromolecules* **1981**, *14*, 1309.
- (21) Fujimura, M.; Hashimoto, T.; Kawai, H. *Macromolecules* **1983**, *15*, 136.
- (22) Xue, T.; Trent, J. S.; Osseo-Asare, K. *J. Membr. Sci.* **1989**, *45*, 261.
- (23) Porat, Z.; Fryer, J. R.; Huxham, M.; Rubinstein, I. *J. Phys. Chem.* **1995**, *99*, 4667.
- (24) Wnek, G. E.; Sheikh-Ali, B. M.; Serpico, J. M.; Ehrenberg, S. G.; Tangredi, T. N.; Karuppaiah, C.; Ye, Y. *Am. Chem. Soc. Prepr., Polym. Div.* **1998**, *39* (1), 54.
- (25) Schroeder, P. *Z. Phys. Chem. (Munich)* **1903**, *45*, 57.
- (26) Zawodzinski, Jr., T. A.; Derouin, C.; Radzinski, S.; Sherman, R. J.; Smith, V. T.; Springer, T. E.; Gottesfeld, S. *J. Electrochem. Soc.* **1993**, *140*, 1041.
- (27) Meyers, J. P. *Simulation and Analysis of the Direct Methanol Fuel Cell*. PhD Dissertation, U. C. Berkeley, 1998.
- (28) Zawodzinski, Jr., T. A.; Gottesfeld, S.; Shiochet, S.; McCarthy, T. J. *J. Appl. Electrochem.* **1993**, *23*, 86.
- (29) Chomakoba-Haefke, M.; Nyffenegger, R.; Schmidt, E. *Appl. Phys. A* **1994**, *59*, 151.
- (30) Lehmani, A.; Durand-Vidal, S.; Turq, P. *J. Appl. Polym. Sci.* **1998**, *68*, 503.
- (31) James, P. J.; McMaster, T. J.; Newton, J. M.; Miles, M. J. *Polymer* **2000**, *41*, 4223.
- (32) Yarusso, D. J.; Cooper, S. L. *Polymer* **1985**, *26*, 371.
- (33) Register, R. A.; Cooper, S. L. *Macromolecules* **1990**, *23*, 318.
- (34) Verma, R.; Hsiao, B.; Biswas, A. *Am. Chem. Soc. Prepr., Polym. Div.* **1998**, *39* (1), 54.
- (35) Quiram, D. J.; Register, R. A.; Ryan, A. J. *Macromolecules* **1998**, *31*, 1432.
- (36) Laurer, J. H.; Winey, K. I. *Macromolecules* **1998**, *31*, 9106.
- (37) Alizadeh, A.; Richardson, L.; Xu, J.; McCartney, S.; Marand, H.; Cheung, Y. W.; Chum, S. *Macromolecules* **1999**, *32*, 6221.
- (38) Magonov, S. N.; Whangbo, M.-H. *Surface Analysis with STM and AFM*; VCH: Weinheim, 1996. Magonov, S. N.; Elings, V.; Whangbo, M.-H. *Surf. Sci. Lett.* **1997**, *375*, L385.
- (39) McLean, R. S.; Sauer, B. B. *Macromolecules* **1997**, *30*, 8314.
- (40) McLean, R. S.; Sauer, B. B. *J. Polym. Sci., Polym. Phys.* **1999**, *37*, 859.
- (41) Brandsch, R.; Bar, G.; Whangbo, M.-H. *Langmuir* **1997**, *13*, 6349.
- (42) Sauer, B. B.; McLean, R. S.; Thomas, R. R. *Langmuir* **1998**, *14*, 3045.

MA000464H